The use of banana leaves and silver particles in the preparation of an absorbent material with unique monarchy / a laboratory study

Amjed Sabeeh obayes

wipoae6d@gmail.com

Abstract:

The primary goal of this research is to create a new material with a successful composition and high monarchy absorption.. This material is prepared by use two main accessories {banana leaves and silver particles} with the use of other secondary accessories .Laboratory experiments were carried out by removing ionstech from {FeIII}, (II) and Pb (II) and use the prepared compound (BLP) / (AgNPs) as adsorbent. The studyer concluded the following: The displacement of ionstech increases in a direct proportion to the rise in (contact time, temperature, agitation speed, and dose of absorbents), and the displacement percentages were 77, 87, and 92 percent, respectively, for (Z., lead, and iron), The 45-minute dumping period. Metal ion binding occurs naturally., practical, and endothermic, as demonstrated by thermodynamic parameters, and as demonstrated by kinetic studies, the process is best characterized by pseudo-second-order kinetics. The adsorption data of Zn(II), Pb(II), and Fe(III) ionstech on (BLP)/(AgNPs) were found to be better represented by the Langmuir isothermal model, with regression coefficients (R = 0.998) and maximum adsorption capacities of 200, 254, and 238 mg/g for Z. (II), lead (II), and iron (III), respectively.

Keywords: green (agricultural) waste, intensive metals, banana tree, ion reduction, silver, absorption

1- Introduction

Without a question, the modern world is experiencing a water crisis, and access to clean water has become a universal demand. Water shortages are caused by pollution, global warming, and the quickening rate of human population development. As a result, it is now essential to use affordable and environmentally friendly technologies as effective means of conserving the world's limited freshwater supplies. [1].

Without a question, the modern world is experiencing a water crisis, and access to clean water has become a universal demand. Water shortages are caused by pollution, global warming, and the quickening rate of human population development. As a result, it is now essential to use affordable and environmentally friendly technologies as effective means of conserving the world's limited freshwater supplies [4]. There is a great danger that trivalent and divalent

intensive metal ionstech, such as $Fe(III), Pb(II)\ and\ Zn(II)$ are indispensable in all spheres of existence. Concentrates of any size can be dangerous to human health because they can enter the food chain and endanger all living forms[6]. The high danger posed by metal ionstech inspires researchers to look for novel ways to safeguard the environment and people using various treatment procedures [7]. Conventional techniques like solvent extraction, electrochemical precipitation, ion exchange, reduction, electrolysis, chemical precipitation, and filtraten have been used, but the majority of these techniques are either ineffective or not economically feasible, especially for low concentrations of intensive metal ionstech [8]. One of the most popular, effective, and affordable techniques for water and wastewater cleaning is adsorption [9, 10]. Several adsorbents, including "clays, polymers, silica, agricultural waste, carbon nanotubes, and activated carbon," have been investigated for the removal of heavy metal ions from waste water [11]. The sorbents made from agricultural wastes have many benefits, including broad availability, environmental friendliness, and technical suitability for a variety of environmental circumstances. (slow absorption and weak affinity for heavy metals), which prompts researchers to look into chemically altering farm waste absorbents[14].

Since they can be grown year-round, bananas are a popular crop. More than 130 nations in the globe cultivate bananas, and millions of tons of bananas are produced worldwide each year[15]; Because it can be a source of sorbent material, banana cultivation refuse should be taken into account. Sieved banana leaf crushed (BLP), which is extracted from homogenized crushed, can be used as an absorbent for wastewater purification. In fact, nanoaccessories have been used as adsorbents in wastewater treatment, and this technology has attracted a lot of interest because of its high efficiency and cheap cost, when compared to the accessories of the old methods [16]. The following variables increase the face reactivity of nanoaccessories:: (1) high face area. (2) the free energy of the raised face. (3) massive to the high number of active sites per unit. These elements render the accoutrements effective adsorbents[17, 18]. Due to their superior adsorbent monarchy, high catalytic activity, and good performance, silver nanoparticles (AgNPs) have been investigated as potential adsorbents.. This is because of their favorable chemical and physical monarchy. They are biocompatible, inexpensive, and highly absorbable[19, 20]. Studies using compounds of silver nanoparticle as adsorbents to extract heavy metal ions and organic pollutants from aqueous solutions suggest outstanding application and high efficacy[21, 22]. However, NPs' poor stability and propensity to aggregate may limit their applicability in wastewater purification[2]. Banana leaf crushed (BLP) is used as mechanical support to hold AgNPs for possible applications in wastewater treatment. (BLP) is a plentiful agricultural waste that is safe for the ecosystem and can be used as an absorbent. [14]. Silver ionstech were fattened into (BLP) by taking advantage of its inherent porosity, followed by the reduction of silver ionstech into silver nanoparticle, with the goal of maximizing the adsorption efficiency, utilizing both (BLP) and (AgNPs), and overcoming the aggregation of AgNPs and avoiding release into solution. Each of the applied (BLP) oxygen nodes (AgNPs) acts as a binding site for AgNPs due to the high abundance of each. [23]. The purpose behind this work was to fabricate $(BLP)/(AgNPs)$

composites with the advantages of both (BLP) and $(AgNPs)$ to remove $Fe(III), Pb(II)\ and\ Zn(II)$ developed by watery solutions tech. The effect of temperature, adsorbent dose, solution pH, and agitation speed on extensive metal ion adsorption was examined as well as several other reaction conditions.

2. The practical side (application)

2. 1. raw accessories

Gamma Laboratory Chemicals supplied the silver nitrate. El Nasr Chemical Company was the supplier of the glucose. (ADWIC, Egypt). Hexahydrates of lead nitrate, zinc nitrate, and ferrous sulphate were purchased from study-lab fine chemical factories. Each of the remedies contained only top-notch substances. used traditional methods and demineralized water to make them.

2. 2. Prepare the required solution

$Zn(II), Pb(II)\ and\ Fe(III)$ In order to make stock solutions, double-distilled water was used to dissolve the necessary amount of mineral salts.. Working solve(50–250 mg/L) were modified by appropriately diluting the standard solution with double-distilled water for the tested metal ions..

2. 3. Crushed banana leaf or shape

After being cleaned with hot distilled water to remove impurities, the gathered banana leaves were allowed to dry for 24 hours before being used as a mechanical support to hold AgNPs while the reduction process was being carried out.

2 . 4. Innovation of silver (nanoparticle) fattened with banana leaves (as crushed)

Silver nanoparticles (AgNPs) were adsorbed on a specific pulverized banana leaf by reducing Ag+ ions in an aqueous solution. AgNO_3 and 1 g of BLP are mixed together in 50 mL of water before glucose solution is added to the reaction mixture. The reaction mixture had a total capacity of 100 ml. AgNO_3 concentration was between 0.00 and 0.07 mol/L, while glucose concentration was 0.05 mol/L. After that, the combination was stirred at 75°C for 45 minutes. A dark brown precipitate that coated the face of the BLP suggested the formation of AgNPs. The finished product was filtered, cleaned with distilled water, and desiccated for two hours at 60 degrees Celsius.. Gaining the absorbance of the reaction mixture through spectral filtering at _(max)14= 420 nm helped to support the generation of AgNPs. The data show that the condensed band at 420 nm is a face plasmon resonance band that developed as a consequence of the activation of free electrons in AgNPs [22].

2. 5. Job description

X-ray refractometer was used to identify the phases of crystals.(XRD, GNR APD-20000 PRO X-ray). Using KBr pellets and a PerkinElmer 1430 spectrometer, (BLP) and (BLP)/(AgNPs) infrared transmittance studies were carried out. A scanning electron microscope was used to study the morphology of BLP/AgNPs. (SEM), TV Joel-JSM-6510.

2. 6. Observations of adsorption

Batch adsorption experiments were applied to remove $Zn(II), Pb(II)\ and\ Fe(III)$ from synthetic solveby a $(BLP)/(AgNPs)$ complex. An $MS-H-Pro$ digital magnetic stirrer with a

PT 1000 temperature sensor and a 2 cm Teflon-coated magnetic stir bar is applied to stir the intensive metal ion $(BLP)/(AgNPs)$ complex solution. A prescribed amount of (BLP)/(AgNPs) synthesized is stirred into a prescribed volume of an intensive metal ion solution at a prescribed starting concentration for a prescribed period of time at a prescribed rate, Using a digital pH meter, the solution's temperature and pH were altered by the adding of either NaOH (0.1 mol/L) or HCl (0.1 mol/L) and recorded. (Model pH System-361, India). One study involved collecting and filtering out 1 ml samples of the chemical reaction of an intense metal ionstech (BLP) solution at regular intervals.(AgNPs) The amount of concentrated heavy metal particles in the filter was measured using an atomic absorption spectrophotometer, model AA55 from the American Varian Corporation. Using Eqs. (1) and (2), it was possible to calculate the displacement rate (R%) and the amount of concentrated metal ions adsorbed per unit mass of adsorbent at time t (q_t).

(2),$q_{\mathrm{e}} = (\mathrm{C}_0 - \mathrm{C}_{\mathrm{e}})\frac{\mathrm{V}}{\mathrm{m}}$ (1)

$$R\% = \frac{(C_0 - C_t)}{C_0} \times 100 \qquad (2)$$

Where, the introductory concentrated of intensive metal ionstech is represented by C_0 ،C_t specifies the concentrated of intensive metal ionstech at time t $(mg\ /\ l)$ ، V is the volume of the solution (L), and m is the massive per gram of the adsorbent.

3. Finding and discussion

3. 1. Profile

3. 1. 1. Diffraction of X-rays

When studying phase and crystal structure, XRD is a trusted fingerprint depiction technique. [24]. The X-ray outcomes are shown in (Figure 1). The BLP peak was found to be associated with the cellulose group crystal plane [25]. Native cellulose, which can be either crystalline or amorphous, is believed to be the primary component responsible for the values obtained for the intense peak at 22.54. [26]. The new compound produced from saturated (BLP)-saturated $(AgNPs)$ can be described crystalline with $AgNPs$ peaky around 20 = 38.3, 45.14 and 64.35, characterizing the refract meter levels of (111), (200), and (220) respectively, AgNPs peaky around = 45.14 and 64.36 indicate that the smaller AgNPs are incorporated into the BLP. In general, the broad and small peaky in the X-ray refractometer pattern are linked to the small particle size. This has to do with how silver is made, which is a face-cubic diamond. Thus, there is unequivocal evidence for the development of Ag nanoparticles stabilized on BLP [27].

3 . 1. 2. An (FT-IR) Spectrum

The usable group of the (BLP) was determined using FTIR spectroscopy, which was also used to show how silver nanoparticles are produced. It facilitates research into the chemistry of synthetic substances. $(BLP)/(AgNPs)$, and consequently the potential reactions between their employable group and intense metal ions[28]. $FT - IR$ spectra of (BLP) and $(BLP)/(AgNPs)$ are seenin Fig.

2. As demonstrated, the presence of an O-H extension group is confirmed by the strong absorption peak at 3420.53 centimeters. (Phenol, alcohol, and carboxylic acid) [29]. The peaky observed at 2910.38 cm^{-1} and 2851 cm^{-1} were assigned to asymmetric C–H clusters and extended symmetric $C-H$ clusters [30]. The peaky at 1732.56 cm^{-1} are the curvature monarchy of the [31] $C=O$ group. The peak at 1519.24 cm^{-1} has been assigned to (C = C)

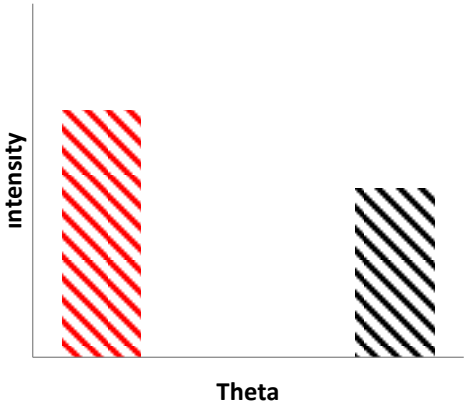

Figure 1 XRD. Spectra of the $BLP\ (BLP)/(AgNPs)$ composite

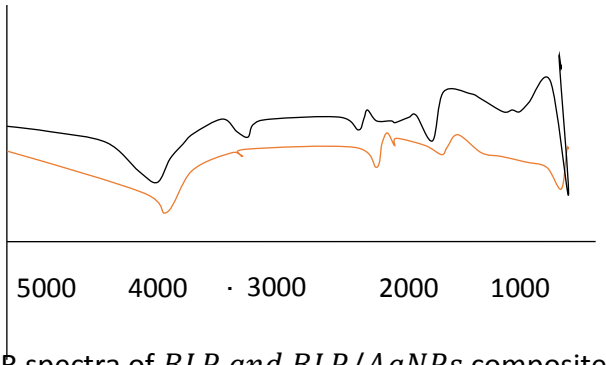

Figure 2. FTIR spectra of $BLP\ and\ BLP/AgNPs$ composite.

Aromatic ring tremor stretching, which is attributed to aliphatic C-H stretching in (CH _3,C - O) stretching, and CH bending at a wavelength of 1380.72 cm-1 [33]. While the band at 1248.23 cm(-1) can be attributed to C-C, C-O, and (C=O) stretching, the band at 1332.58 cm depicts the (C-C) and (C-O) ring stretching shakings [33]. [34] Additionally, peaky at 896 cm-1 and 655 cm-1 are ascribed, respectively, to the C-H rocking shakings of the cellulose group and the (C-O-H) group. As a result, following impregnation with (AgNPs, AgNPs), the bands have been effectively loaded as shown by the disappearance of some peaks and changes in the intensity of some bands. (BLP). These functional groups may make it easier for powerful metal ions to be absorbed.

3 .1. 3. Compound Morphology

SEM image depiction is a technique applied to gain the face morphology of the generated adsorbent ($BLP/AgNPs$). the $AgNPs$ (white spots) clearly have a quasispherical shape and uniform size distribution. The AgNPs adhered well to the BLP face due to the silver's high affinity for oxygen and nitrogen in the BLP workable group[22]

3 . 2. The impact of adsorption of intensive metal ionstech on the reaction coefficients

The (BLP)/(AgNPs) complex was studied in adsorption studies to remove Zn (II), Pb (II), and Fe (III) ions from aqueous solutions. The contact time, initial intensive metal ion concentration, temperature, adsorbent dose, agitation speed, and solution pH were all varied during the adsorption process. Each parameter's unique effect is methodically analyzed and researched.. The experimental finding showed the expected sensitivity of $Zn\ (II), Pb\ (II), and\ Fe\ (III)$ ionstech Each metal ion's precedence in an aqueous solution depends on the pH. The following are the ideal circumstances for experimentstech: Except where otherwise noted, the following conditions were used: 0.1 g of adsorbent, 100 ppm of metal ions, 300 rpm of stirring, 0.1 L of aqueous solution at 30°C, pH = 5 (for Zn(II)L), and pH = 6 (for Pb(II) and Fe(III) ionstech).

3. 2. 1. period of contact's effect

All other factors were held constant while analyzing the effect of contact time on the (50-250 ppm) adsorption of Zn(II), Pb(II), and Fe(III) ions on (BLP/AgNPs). Figure 3 depicts the effect of contact duration on the percentage displacement of the initial 50 ppm Zn(II), Pb(II), and Fe concentrate.(III). The percentage of $Zn(II), Pb(II), and\ Fe(III)$ ionstech removed at time t increased sharply with time and reached a plateau after about 35 min. Approximately 70%, 70%, and 75% of the $Zn(II), Pb(II), and\ Fe(III)$ ionstech are removed after 35 minutes of stirring, respectively. The efficiency of the metal ionstech's adsorption rises with longer contact times. The amount of time needed for Zn(II), Pb(II), and Fe movement at equilibrium (I I I) Ionstech was determined to be 35 minutes because the adsorption efficiency declines as contact time rises up to 120 minutes. The BLP/AgNPs adsorbent mainly employs the intraparticle diffusion model and intricate adsorption processes when adsorbing Zn (I I), Pb (I I), and Fe (I I I) ions [36]. Due to the availability of active sites on the surface of (BLP), the rate of adsorption of Zn (I I), Pb (I I), and Fe (I I I) ions increased quickly during the initial period.(AgNPs). As a result, as vacant sites for uptake became less and less available over time, the uptake of intensive metal ionstech reduced.

3. 2. 2. The impact of the dose of the adsorbent

Adsorbent dose quantity and adsorbent/solution rate have a significant impact on adsorption efficiency in the batch adsorption technique. [37]. Figure 4 shows The displacement rates of $Zn(II), Pb(II)\ and\ Fe(III)$ ionstech were gained with different doses of $BLP/AgNPs$ and fixed metal ion concentrates.. , the displace men percentage increased from (73–95%), (84–100%), and (86–100%) for $Zn(II), Pb(II), and\ Fe(III)$ ionstech, respectively. by boosting the BLP/AgNPs dosage from 0.05 to 0.25 g. This behavior may be caused by the increased adsorbent used in the

adsorption process, the larger surface area, and the consequent increase in the number of ionstech exchange sites accessible [38].

3.2.3. Impact of introductory$Zn(II), Pb(II)$ and $Fe(III)$ concentratens

The initial concentrations of Zn(II), Pb(II), and Fe(III) ions were changed between 60 and 260 ppm at a fixed dose in order to study the effects they had on the adsorption reactions. (0.1) g of $BLP/AgNPs$. Figure 5 shows that the displacement rate of $Zn(II), Pb(II)$ and $Fe(III)$ ionstech decreases with increasing introductory concentrated from (84-60%), (90-73.6%) and (98-76%), although respectively, such as metal ionstech

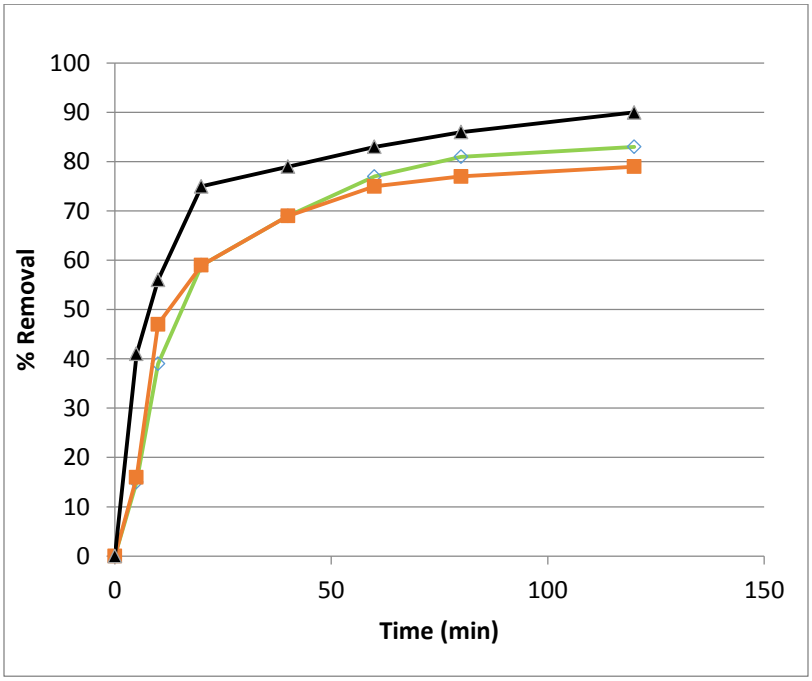

Fig 3. Contact time's effect on Zn displacement rate$(II), Pb(II)$ and $Fe(III)$ ionstech on $BLP/AgNPs$

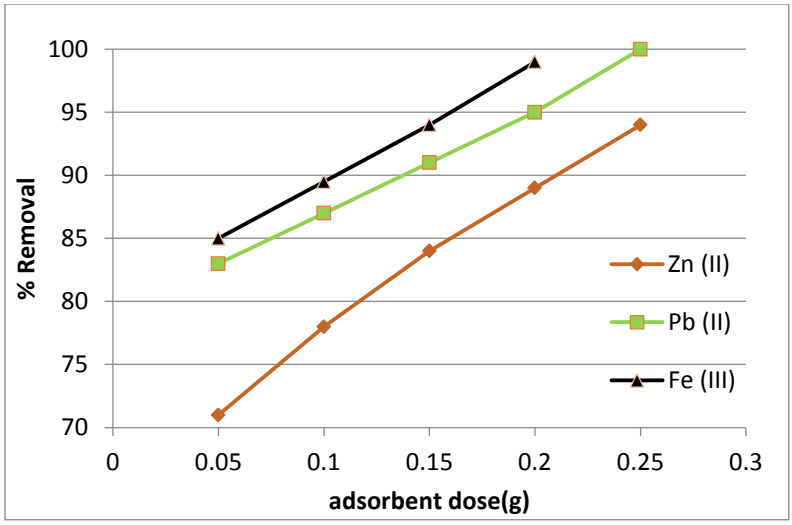

Fig. 4. Adsorbent dose's effect on Zn displacement rate (II), $Pb\ (II), and\ Fe\ (III)$ ionstech

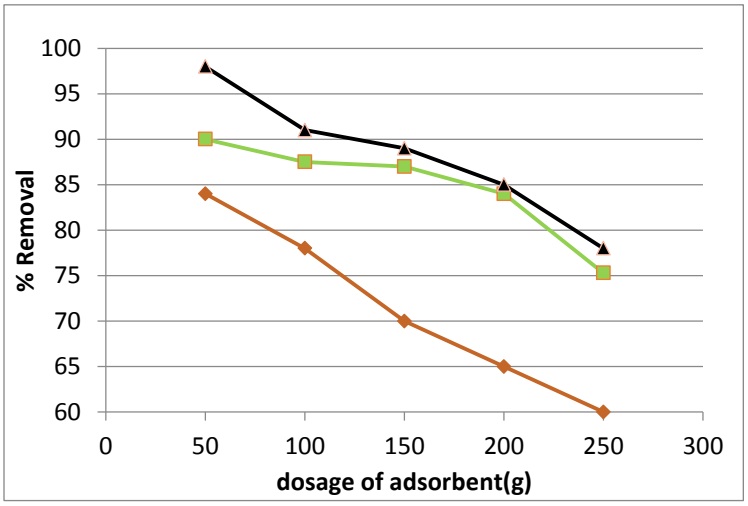

Fig. 5. Impact of metal ion concentrated on the displacement rate of $Zn\ (II), Pb\ (II)\ and\ Fe\ (III)$ ionstech

The concentrated increases from (55 to 255) ppm. The concentrated-dependent displacement percentage of elemental metal ionstech may be due to the existence of abundant active adsorption sites on the face of ($BLP/AgNPs$) with low concentrates of metal ionstech, and the face of free $BLP/AgNPs$ of metal ionstech, but at high concentrates, there are few active sites on The face of $BLP/AgNPs$ that prevent additional metal ions from being absorbed into the

3. 2. 4. Impact of Temperature

The results of the experiment supported the hypothesis that temperature has a substantial effect on the ability of (BLP/AgNPs) to adsorb Zn(I I), Pb (I I), and Fe (I I I) ions from aqueous solutions. The temperatures used for the adsorption experiments ranged from 25 to 40 degrees Celsius. Figure 6 demonstrates that the amount of Zn(I I), Pb (I I), and Fe(I I I) ionstech removed by (BLP / AgNPs) increases from (70-86%), (82-96%), and (82-95%), respectively, as the

temperature raises from 25 to 50 °C. Better Zn (II), Pb (II), and Fe(I I I) ion displacement occurs at higher temperatures, which can be ascribed to the increased rate of sorbate diffusion within the adsorbent's pores and the reduced viscosity of the liquid [40]. The reaction behavior supports the adsorption process' endothermic character.

3. 2. 4. 1. thermodynamic indicators. The thermodynamic behavior of adsorption of $Zn\ (II), Pb\ (II)\ and\ Fe\ (III)$ ionstech on the face of $(BLP/AgNPs)$ Indicators that can be used to describe shifts in energies include Gibbs free energy change (G°), enthalpy change (H °), and entropy change. (S°) determined by Eq (3).

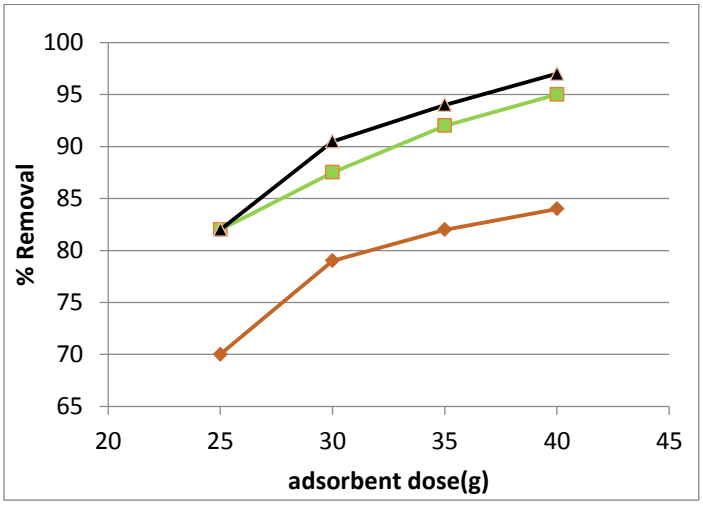

Fig. 6 . Impact of temperature on the displacement rate of $Zn\ (II), Pb\ (II), and\ Fe\ (III)$ ionstech

$$\Delta G° = -RTLnK_C \qquad (3)$$

where R is the gas constant (8.314 J/mol K) and K_(c) is the solute distribution coefficient, which is equal to q _(e) / C_e. The equation makes use of the values of K_(c). (3) Calculating (G°), (H°), and (S°) using Eq (4).

$$(\Delta G°) = (\Delta H°) - (T\ \Delta S°) \qquad (4)$$

Equation (Eq.), which gives the Van't Hoff equation, can be used to determine the values of other thermodynamic parameters (5).

$$lnK_C = \frac{(\Delta S°)}{R} - \frac{(\Delta H°)}{(RT)} \qquad (5)$$

By determining the slope and intercept, thermodynamic parameters were derived from linear van't Hoff plots (lnK_C vs 1/T). (Fig. 6). The results are summarized in Table 1, and positive values of H and S show endothermic adsorption of Zn (II), Pb (I I), and Fe (I I I) ions on (BLP/AgNPs) and increased randomness at the solid/solution interface, respectively. Negative values of G° encouraged the natural and practicable adsorption of Zn (I I), Pb (I I), and Fe (I I I) ions [41].

3. 2. 5 . Impact speed of Agitation

The rate of agitation in a reaction mixture, an inherent factor affecting the adsorption process, impacts the dispersion of the reactants.., the affinity of adsorbents/adsorbents, and massive transfer. the shape 9

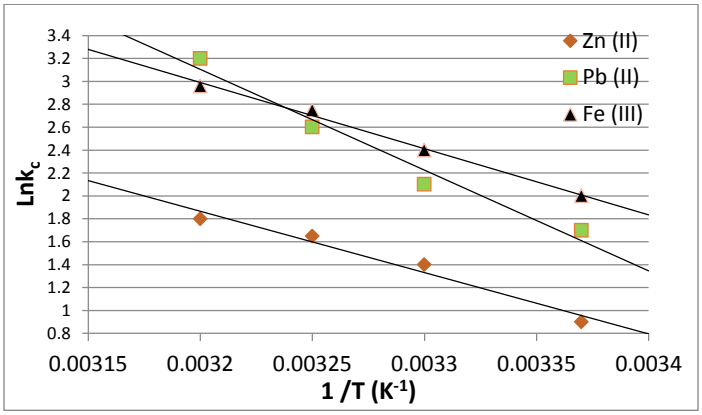

Figure7. Plot showing the temperature range's relevant 1/T and ln K_(c) values.

Table 1. Thermal absorption indices for: 1) *Zinc (II); lead (II);) and iron (III)*

			ΔG		**K**	
(Metal) (ion)	(ΔH°) Jmol $^{-1}$	ΔS° $Jmol^{-1}K^{-1}$	299	304	309	314
Zn(II)	695	2.55	- (2099.3)	- (3337.7)	- (4246.3)	- (4724.9)
Pb (II)	1196.9	4.12	- (3766.9)	- (5018.3)	- (6624.8)	- (8271.3)
Fe (III)	829	2.99	- (4498.6)	- (5829.4)	- (7046.8)	- (7663.3)

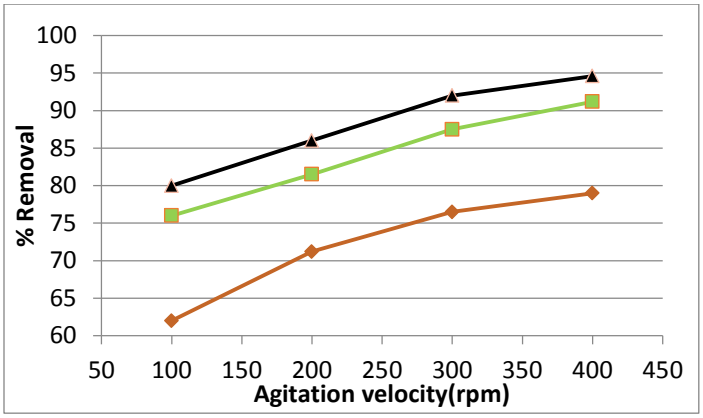

Figure 8. agitation speed's effect on the displacement rate of zinc $(II), Pb\ (II), and\ Fe\ (III)$ ionstech

Results from experiments on the effects of agitation rates of (100, 200, 300, and 400) rpm on the adsorption of Zn.(II), $Pb(II)$ and $Fe(I\ I\ I)$ ionstech on the face of $BLP/AgNPs$, in other fixed limits. The displacement efficiencies increased from (63–82%), (76–92%) and from (80–94%) $Zn(II), Pb(II)$ and $Fe(I\ I\ I)$, respectively, with increasing agitation speed. . Increases in the diffusion rates of Zn(II), Pb (I I), and Fe (I I I) ions in the bulk solution, a decrease in the boundary layer, and an increase in the rate of ion transport in the solution might all be contributing factors to the displacement rate increasing [42], while the agitation speed Slow water may cause adsorbed particles to accumulate in the solution.

3 .2 .6. PH effects in solutions

Solution By affecting the solution chemistry of intensive metals and the face charge density of the adsorbent, pH significantly affects the adsorption of intense metal ions. [43]. The impact of pH on the displacement of $Zn(II), Pb(II)$ and $Fe(III)$ ionstech by the $BLP/AgNPs$ complex was investigated, and the finding are seenin. Because at exponential values, the adsorption process was examined at pH 7. Real adsorption experiments are restricted by the formation of insoluble metal hydroxides at higher pH levels caused by intense metal ions[44]. Figure 9 shows that the displacement percentage increased as a function of pH for Z. (I I), lead (II), and iron (III) ionstech from (27-77%), (23-88%), and (30-91%), respectively. At pH (5) and pH (6), respectively, the displacement percentages with Zn (I I), Pb (I I), and Fe (I I I) ionstech reached highest values of 79%, 88%, and 91%. Low pH causes hydrogen ions to compete with metal ions for binding sites on the surface of BLP/AgNPs, which results in greater adsorption and displacement efficiencies for metal ions[45]. On the other hand, as pH increases, the competition between protons (H+) and positively charged metal ions at the face sites diminishes, leading to an increase in displacement rate. At neutral pH levels or higher, high adsorption efficiencies for the BLP/AgNPs adsorbent are expected; however, strong metal ions may precipitate as insoluble metal.

The real evaluation of the adsorption process is restricted by hydroxides above pH 6 [46]. By forming a complex, metal ions can create a stable and strong bond with the workable group on the surface of BLP/AgNPs. The current adsorbents demonstrated high Zn (I I), Pb (I I), and Fe (I I I) ion According to the experimental results, the adsorbents produced from agricultural waste have lower displacement efficiencies and higher adsorption capacities.

3 . 3 Isotherms of Adsorption

Adsorption isotherms are used to explain how the solution and adsorbate are distributed during equilibrium adsorption and to pinpoint the mechanism underpinning the adsorption process. [47]. Three isothermal models—Langmuir, Freundlich, and Temkin—were used to evaluate the data obtained from the adsorption of Zn (I I), Pb (I I), and Fe (I I I) ions on (BLP/AgNPs). The Langmuir adsorption isotherms presumptively adsorb uniform sides and monolayers. The Langmuir absorption is defined by Eq(6).

$$\frac{C_e}{q_e} = \frac{1}{K_L\, q_m} + \frac{C_e}{q_m} \qquad (6)$$

q_e is the capacity of the adsorption process at equilibrium (mg/g), q_mis is the maximal active site capacity (mg/g), and K_L (L mg(-1)) is the Langmuir constant to calculate the adsorption energy. where C_e is the equilibrium concentration of the element in solution (mg/L). As seen in Fig. 9, by plotting the association stechhip C_e / q_evs. C_e, the values of q_m and KK_L can be ascertained from the slope and intercept of the graphs.

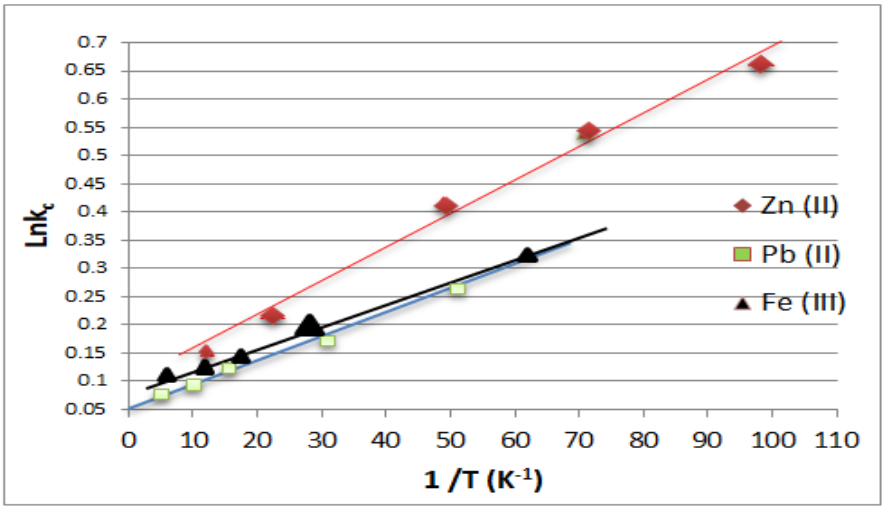

Figure 10. Langmuir adsorption isotherms of $Zn(II), Pb(II), and\ Fe(III)$ ionstech on the face of $BLP/AgNPs$

; Table 2 provides a summary. The dimensionless separaten factor (R_L) provided by Eq. (7) served as a proxy for the affinity between the adsorbent and the adsorbent in the Langmuir isothermal model;

$$R_L = \frac{1}{1 + K_L C°} \qquad (7)$$

The initial metal ion condensed (mg/L) is represented by Co. When its values are between zero and one, the R-L value characteristics show that the nature of adsorption is advantageous. A favorable adsorption interaction stech is indicated by the estimated R_L values for the adsorption of Zn(I I), Pb.(I I), and Fe.(I I I) ionstech on (BLP/AgNPs), which are, respectively, (0.39, 0.29), and 0.2 at 50 mg L(-1). A heterogeneous face and multilayer adsorption are the foundations of the practical Freundlich equation. Eq. can be used to determine the Freundlich isotherm's linear shape.(8).

$$\ln q_e = \ln K_F + \left(\frac{1}{n}\right) \ln C_e \qquad (8)$$

where K_(F) and n, which are determined by the intercept and regression of the lnq_(e) vs. lnC_(e) plot shown in Fig. 11, are, respectively, adsorption capacity and adsorption strength. The resulting 1/n values shown in Table 2 support BLP/AgNPs' substantial adsorption capability. The

Temkin isotherm includes a component that accounts for the heat of adsorption reaction stitch and assumes a uniform distribution of binding energies [48]. Eq provides the shape in a linear form.(9),

$$q_e = B_t \ln A + B_t \ln C_e \quad (9)$$

The equation (B-t = RT/ b), where b is the heat of absorption (J/mol) and A is the equilibrium constant connected to the maximal binding energy (l/g), can be used to visualize a histogram of q_e vs. lnC_e. Absolute temperature (K) and the gas constant (8.314 J / mol K) are denoted by the letters T and R, respectively. (Fig. 12) and Table 2 contains the values of the isothermal constants that were given. With correlation coefficient values close to unity, it was determined that the Langmuir isotherm was the best model for explaining the adsorption of Zn (I I), Pb (I I), and Fe (I I I) ions on the surface of (BLP/AgNPs) based on the adsorption coefficients discovered in Table2.

The Langmuir isotherm and the experimental findings concur, which points to a consistent face and monolayer coverage. To determine whether BLP/AgNPs is a suitable adsorbent, its adsorption capacity is investigated. The Langmuir isotherm and experimental findings agree, which points to uniform face and monolayer coverage. In order to evaluate BLP/AgNPs as an adsorbent, its adsorption capacity was compared to that of other previously investigated adsorbents listed in Table 3. Previous studies addressed using banana leaves as adsorbents and showed that they had a moderate capacity for adsorption [49], There was a critical need to boost the absorption of available, cheap sorbents as a result. (banana leaves). In this research, AgNPs were added to the faces of banana leaves to increase their capacity for adsorption. All of the metal ions and impurities that are presently present are removed using the novel BLP/AgNPs adsorbent compound, which is also a suitable fine adsorbent for various effluents and wastewater.

Table 2. Isotherms data of ionstech onto face.

Adsorption isotherm	Parameters	Values / metal ionstech		
Langmuir		0.033	0.06	0.07
		191 mg	245 mg	229 mg
		0.996	0.994	0.998
Freundlich		16.3 mol	22 mol	30.6 mol
		0.5	0.56	0.48
		0.98	0.97	0.999
Temkin		42.7 J	59 J	50 J
		0.98	0.98	0.98

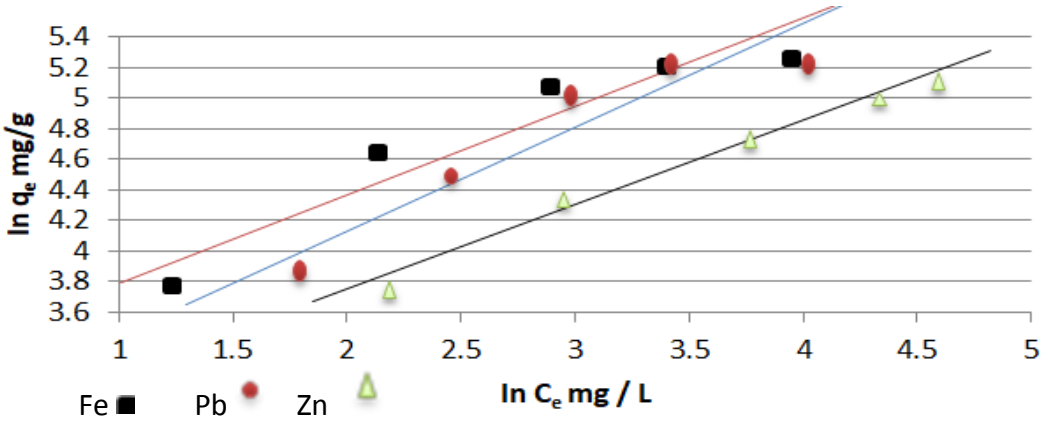

Fig 11. The Freundlich isotherm for the absorption of Zn (I I), Pb (I I), and Fe (I I I) ions on BLP/AgNPs face.

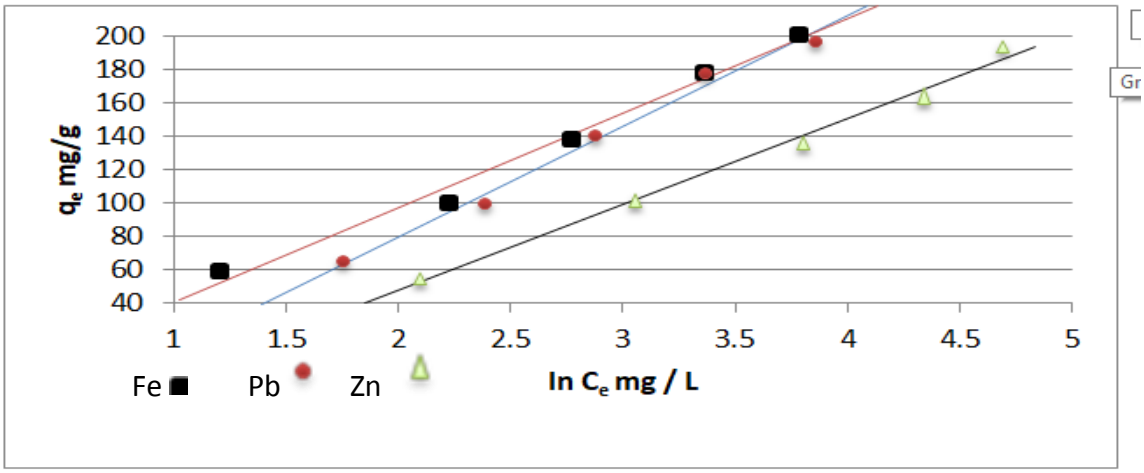

Figure 12 shows the Temkin isotherm for the deposition of Zn (I I), Pb (I I), and Fe (I I I) ions onto the face of BLP/AgNPs.

Table3. Adsorption capacities for ionstech to other previously studied .

Adsorbent	Metal ionstech as an adsorbate, (mg/g)			References
BLP/AgNPs	209	268.4	250.8	This study
flax/ fibres	9.2983	11.8151		51.1
Albizia lebbeck pod(s)	9.086	7.887		52.1
manganese dioxi	24.618		77.737	53.1
bael/ leaves		137.5		54.1
bael/ leaves	1.98		3.08	55.1

3. 4. Kinetics of Absorption

to understand binding patterns better; To predict the rate of Zn (I I), Pb (I I), and Fe (I I I) ion adsorption on the surface of (BLP/AgNPs), whether through a chemical reaction or a massive transfer, numerous kinetic models have been used.

3. 4. 1. The kinetic paradigm of pseudo-first order

Assuming that the number of open adsorption sites is inversely proportional to the displacement rates of heavy metal ions, this model explains the adsorption rate based on the adsorption capacity [55]. A general formulation of the first-order Lagergren form is given by equation (10).

$$\log (q_e - q_t) = \log q_e - \left(\frac{k_1}{2.302}\right) t \qquad (10)$$

where q_e and q_t represent, respectively, the equilibrium and time-dependent amounts of concentrated metal ionstech deposited on the surface of (BLP/AgNPs). (min). The slope and curve of the parabola (q_e-q_t) vs. t are used to calculate the equilibrium capacity and pseudo-first-order kinetic constant, respectively. (not shown). The final numbers for q_e, k_1, and R2 are shown in Table 4. Kinetic theory The adsorption of Zn(II), Pb(II), and Fe(III) ions on BLP/AgNPs cannot be explained by false first class because the calculated values of q_e were very different from the experimental values.

3.4.4. The kinetic paradigm of pseudo-second order

Metal ions that are equilibrium-adsorbed on the surface of the adsorbent at time t are measured using a pseudo-second-order process [56, 57]. as shown by Eq .(11);

$$\frac{t}{q_t} = \frac{1}{k_2 \, q_e^2} + \frac{t}{q_e} \qquad (11)$$

To identify variables like k_2, q_e, and R2, plots of t/q_t vs. t (not shown) are used. The intercept and slope of the plot were used to determine the second-order rate constant k_2 (g mol(-1) min(-1)) and q_e (mg/g)f, which are both shown in Table 4. Introductory(h) was given to the absorption rate with the calculated values of k_2 and q_e specified by Eq.(12)

$$h = k_2 q_e^2 \qquad (12)$$

The second-order model is consistent with the adsorption of Zn (II), Pb (II), and Fe (II I) ions on the surface of the (BLP/AgNPs), as evidenced by the high correlation coefficient that is close to unity R2=0.999 and the satisfactory fit of the kinetic data to the obtained experimental findings.

3. 4. 3. Model for intraparticle diffusion

Because the diffusion mechanism could not be found using earlier pseudo-second-order models, Weber and Morris created an intraparticle diffusion model to study the stages of the diffusion mechanism and the characteristics of the rate-limiting step. [58]. The intraparticle flow is provided by Eq.(13),

$$q_t = k_p \, t^{0.5} + C \qquad (13)$$

where the number of metal particles, q_t (mg g (-1)), is present. At time t, Zn(II), Pb(II), and Fe(III) adsorbed as k_(p) (mg/g min(0.5)), respectively, on adsorbents (BLP/AgNPs). , Pb(II), and Fe(II), which were deposited on (BLP/AgNPs), indicate the intraparticle speed limits, and C represents the breadth of the boundary layer that was produced. The intraparticle diffusion plot (not shown) demonstrates the existence of two distinct phases in the adsorption process. The explanation of the exterior face's absorption appears in the first linear section. In the second phase, which is shown by the second linear section in Table 5, Zn(II), Pb(II), and Fe(II) ions gradually adsorb inside the pores of the BLP/AgNPs particles. The rate values for stages k_(p1) and k_ are given.(p2). The figure also deviates from the origin, demonstrating the use of additional kinetic models to regulate the adsorption of Zn (II), Pb (II), and Fe (II I) ions as well as the fact that intraparticle diffusion is not the only factor affecting rate.[59].

3. 4. 4. Interaction mechanism

The Zn (I I), Pb (I I), and Fe (I I I) ionstech adsorption mechanisms on the (BLP/AgNPs) hybrid may be caused by the physical adsorption and/or precipitation of metal ions. Additionally, it is suggested that chemisorption as well as the intricate electrostatic interplay between the positively charged metal ionstech and silver nanoparticle (Ago) may all be involved in the metal ionstech's adsorption.

Table 4. Models for the adsorption of ions onto surfaces using adsorption rates

Metal ion			Model of pseudo-first order			Model of pseudo-second order		
	mg/l							
Zn (II)	55	46.2	30.3	7.59	1.078	49.72	2.42	1.0989
	110	86.9	61.2	6.831	1.089	95.04	1.001	1.0989
	165	116.6	66.9	4.84	1.045	123.2	1.1	1.0989
	220	141.9	84.6	4.4	1.045	151.8	0.891	1.0989
	275	165	104	3.3	1.023	173.8	0.803	1.0978
Pb (I I)	55	49.5	35.3	4.18	1.067	55.22	1.54	1.0989
	110	96.8	54.9	5.72	1.056	103.84	1.32	1.0989
	165	144.1	82.3	5.61	1.045	150.37	0.869	1.0967
	220	181.5	107	7.48	1.078	190.63	0.825	1.0978
	275	202.4	114	4.29	1.045	210.76	0.902	1.0989
Fe (I I I)	55	51.7	31.7	7.37	1.045	54.56	2.75	1.0989
	110	100.1	63.5	7.37	1.078	106.37	1.21	1.0989
	165	146.3	80.7	7.15	1.0747	149.38	1.166	1.0989
	220	182.6	98.8	5.72	1.045	188.65	1.034	1.0989

	275	209	113	7.04	1.078	217.36	0.99	1.0989

Table 5. Intraparticle diffusion

Metal ion	mg/l	Intraparticle mode			
Zn(II)	55	3.3	1.078	0.682	1.067
	110	5.28	1.089	1.76	1.078
	165	6.05	1.078	2.31	1.034
	220	6.71	1.089	2.53	1.034
	275	7.48	1.078	3.19	1.067
Pb(II)	55	7.26	1.089	1.65	1.078
	110	10.67	1.089	3.63	1.045
	165	13.09	1.089	4.07	1.078
	220	13.53	1.089	4.73	1.034
	275	16.83	1.078	6.93	1.067
Fe(III)	55	7.26	1.089	1.54	1.078
	110	10.67	1.089	3.63	1.045
	165	13.09	1.089	4.07	1.078
	220	13.53	1.089	4.73	1.034
	275	16.83	1.078	6.6	1.067

development of decreased metal ions. According to Eqs. (14), and complications and reduction could happen. (15),

$$\mathrm{A\,g^{\circ}{}_{m}} + \left(\frac{m}{2}\right)(\mathrm{Zn^{2+}}) \longrightarrow (\mathrm{mAg^{+}} + (\mathrm{m}/2)\,\mathrm{Z\,n^{\circ}} \qquad (14)$$

$$\mathrm{Ag^{\circ}{}_{n}} + (\mathrm{Zn^{2+}}) \longrightarrow \mathrm{Ag^{\circ}{}_{(n-2)}Zn^{\circ}} + (2\mathrm{Ag^{+}}) \qquad (15)$$

Workable group on BLP faces may contribute to the adsorption of $Zn(II), Pb(II), and\ Fe(III)$ ionstech as H-metal ion exchange, adsorption of metal-ion face complexes, or both. According to Eq., there may be intense metal ion adsorption.(16),

$$(\mathrm{BLP}/\mathrm{AgNPs}) + (\mathrm{Fe^{3+}\ aq}) \rightarrow (\mathrm{Fe^{3+}}) - (\mathrm{B\,LP}/\mathrm{AgNPs}) \qquad (16)$$

The results of the laboratory studies supported the idea that increasing pH enhances the adsorption of strong metal ions, which is inhibited in an acidic medium.

4. Conclusion

The focus of the research was on creating an effective and reliable test material (test) of composition (3), validating impregnation and X-ray refractometer (XRD) patterns, and analyzing raw infrared accessories using the Fourier transform. Fe (III) from aqueous solutionstech, and the

experimental studyer discovered that the adsorption conditionstech and the adsorption can with the increase of both (1) contact time had a substantial impact on the adsorption of Zn (I I), Pb (I I), and Fe (I I I) ions. (2) The adsorbent's dosage. (3) Temperature and the rate of movement. (4) The pH of the solution was controlled during the mineral adsorption, and the maximum adsorption was obtained at pH 7 for the Zn(I I) ion and pH 8 for the Pb (I I) and Fe (I I I) ions. The absorption of Zn(II), Pb(II), and Fe (I I I) ions follows the intraparticle diffusion model and the pseudosecondary system's kinetics. The prepared material will also be helpful in a number of industries and for treating liquid waste.

Sources

[1] S.K. Pradhan, J. Panwar, S. Gupta, Enhanced intensive metal displacementusesilveryttrium oxide nanocomposites as novel adsorbent system, J. Environ. Chem. Eng. 5(6) (2017) 5801–5814.

[2] K.O. Shittu, O. Ihebunna, Purification of simulated waste water usegreen synthesized silver nanoparticle of Piliostigma thonningii aqueous leave extract, Adv. Nat. Sci. Nanosci. Nanotechnol. 8 (4) (2017), 045003.

[3] R.S. Dubey, R. Xavier, Study on displacementof toxic metals usevarious adsorbents from aqueous environment: a review, Sci. J. Eng. 1 (1) (2015) 30–36.

[4] F. Ge, M.M. Li, H. Ye, B.X. Zhao, Impactive displacementof intensive metal ionstech $Cd^{+2}, Zn^{+2}, Pb^{+2}, Cu^{+2}$from aqueous solution by polymer-modified magnetic nanoparticle, J. Hazard Mater. 211 (2012) 366–372.

[5] X. Wang, Y. Guo, L. Yang, M. Han, J. Zhao, X. Cheng, Nanoaccessories as sorbents to remove intensive metal ionstech in wastewater treatment, J. Environ. Anal. Toxicol. 2 (7) (2012) 154.

[6] S. Afroze, T.K. Sen, A review on intensive metal ionstech and dye adsorption from water by agricultural solid waste adsorbents. Water, Air, Soil Pollut. 229 (7) (2018) 1–50.

[7] A. Ali, A. Mannan, I. Hussain, I. Hussain, M. Zia, Impactive displacementof metal ionstech from aquous solution by silver and Z. nanoparticle workableized cellulose: isotherm, kinetics and statistical supposition of process, Environ. Nanotechnol. Monit. Manag. 9 (2018) 1–11.

[8] A.G.B. Pereira, A.F. Martins, A.T. Paulino, A.R. Fajardo, M.R. Guilherme, M.G.I. Faria, E.C. Muniz, Recent advances in designing hydrogels from chitin and chitin-Derivatives and their impact on environment and agriculture: a, Rev. Virtual Quim 9 (2017).

[9] I. Ali, V.K. Gupta, Advances in water treatment by adsorption technology, Nat. Prot. 1 (6) (2006) 2661–2667.

[10] G. Chauhan, P.U.K. Chauhan, Risk assessment of intensive metal toxicity through contaminated vegetables from waste, Int. J. Adv. Technol. Eng. Sci. 51 (2014) 444–460.

[11] O. Hakami, Y. Zhang, C.J. Banks, Thiol-workableised mesoporous silica-coated magnetite nanoparticle for high efficiency displacementand recovery of Hg from water, Water Res. 46 (12) (2012) 3913–3922.

[12] M.K. Uddin, A review on the adsorption of intensive metals by clay minerals with special focus on the past decade, Chem. Eng. J. 308 (2017) 438–462.
[13] A. Gupta, S.R. Vidyarthi, N. Sankararamakrishnan, Enhanced sorption of mercury from compact fluorescent bulbs and contaminated water streams useworkableized multiwalled carbon nanotubes, J. Hazard Mater. 274 (2014) 132–144.
[14] V.K. Gupta, A. Nayak, S. Agarwal, Bioadsorbents for remediation of intensive metals: current status and their future prospects, Environ. Eng. Res. 20 (1) (2015) 1–18.
[15] fao, Banana Market Review and Banana Statistics 2012–2013. Market and Policy Analyses of Raw Accessories, Horticulture and Tropical (RAMHOT) Products Team. Rome, 2014.
[16] K.M. Al-Qahtani, Cadmium displacementfrom aqueous solution by green synthesis zero valent silver nanoparticle with Benjamina leaves extract, Egypt. J. Aqua. Res. 43 (2017) 269–274.
[17] Y. Zhang, B. Wu, H. Xu, H. Liu, M. Wang, Y. He, B. Pan, Nanoaccessories-enabled water and wastewater treatment, NanoImpact 3 (2016) 22–39. .
[18] S.T. El-Wakeel, R.S. El-Tawil, H.A. Abuzeid, A.E. Abdel-Ghany, A.M. Hashem, Synthesis and structural monarchy of MnO_2 as adsorbent for the displacementof lead (Pb^{+2}) from aqueous solution, J. Taiwan Inst. Chem. Eng. 72 (2017) 95–103.
[19] S.G. Kim, N. Hagura, F. Iskandar, K. Okuyama, Depictionof silica-coated Ag nanoparticle synthesized usea water-soluble nanoparticle micelle, Adv. Crushed Technol. 20 (2009) 94–100
[20] Oubagaranadin, J.U.K., and Murthy, Z.V.P., "Adsorption of divalent lead on a montmorillonite illite type of clay", Ind Eng Chem Res, vol.48, pp.10627-10636, 2009.
[21] Sun, S., Wang, L., and Wang, A., "Adsorption monarchy of crosslinked carboxymethyl chitosan resin with Pb(II) as template ionstech", J Hazard Mater, vol.136, pp.930-937, 2006.
[22] Wang, X., Zheng, Y., and Wang, A., "Fast displacementof copper ionstech from aqueous solution by chitosan-g-poly (acrylic acid)/attapulgite composites", J Hazard Mater, vol.168, pp.970-977, 2009.
[23] Gao, C., Zhang, W., Li, H., Lang, L., and Xu, Z., "Controllable
of mesoporous MgO with various morphologies and their absorption performance for toxic pollutants in water", Cryst Growth Des, vol.8, pp.3785-3790, 2008.
[24] Lee, J., Mahendra, S., Alvarez, P.J.J., "Nanoaccessories in the construction industry: A review of their applicationstech and environmental health and safety consideratens", ACS Nano, vol.4, pp.3580-3590, 2010.
[25] Xu, X., Wang, Q., and Choi, H.C., "Encapsulation of iron nanoparticle with PVP nanofibrous membranes to maintain their catalytic activity", J. Membr. Sci, vol.348, pp.231–237, 2010.
[26] Wang, Q., Qian, H.J., Yang, Y.P., Zhang, Z., Naman, C., and Xu, X.H., "Reduction of hexavalent chromium by carboxymethyl cellulose-stabilized zero-valent iron nanoparticle", J. Contam. Hydrol, vol.114 (1–4), pp.35–42, 2010.

[27] Xiong, Z., Zhao, D., and Pan, G., "Rapid and complete destruction of perchlorate in water and ion-exchange brine usestabilized zero-valent iron nanoparticle", Water Res, vol.41 (15), pp.3497–3505, 2007.
[28] Liu, T., Zhao, L., Sun, D., and Tan, X., "Entrapment of nanoscale zero-valent iron in chitosan beads for hexavalent chromium displacementfrom wastewater", J. Hazard. Mater, vol.184 (1–3), pp.724–730, 2010.
[29] Liu, Z., and Zhang, F., "Nano-zerovalent iron contained porous carbons developed from waste biomassive for the adsorption and dechlorination of PCBs", Bioresour. Technol, vol.101 (7), pp.2562–2564, 2010.
[30] Ponder, S.M., Darab, J.G., and Mallouk, T.E., "Remediation of Cr(VI) and Pb(II) aqueous solveusesupported nanoscale zero-valent iron", Environ, Sci. Technol, vol.34 (12), pp.2564–2569, 2000.
[31] Lin, C.J., Liou, S.L., and Lo, Y.H., "Degradation of aqueous carbon tetrachloride by nanoscale zerovalent copper on a cation resin", Chemosphere, vol.59, pp.1299–1307, 2005.
[32] Wu, S.J., Liou, T.H., and Mi, F.L., "Synthesis of zero-valent copper-chitosan nanocomposites and their application for treatment of hexavalent chromium", Bioresour. Technol, vol.100 (19), pp.4348–4353, 2009.
[33] Bassett, G.H., Jeffery, J., Mendham, J., and Denney, R.C., Vogel"s Text Book of Quantitative Chemical Analysis, fifth ed., Longman, London,1989. [34] Sosa, I.O., Noguez, C., and Barrera, R.G., "Optical monarchy of metal nanoparticle with arbitrary shapes", J. Phys. Chem, vol.107, pp.6269– 6275,2003. [35] Suman, T.Y., Radhika Rajasree, S.R., Kanchana, A and Beena, S., "Elizabeth Biosynthesis, depictionand cytotoxic impact of plant mediated silver nanoparticle useMorinda citrifolia root extract", Colloids Surf B, vol.106, pp.74– 78, 2013. [36] Sankar, R., Karthik, A., Prabu, A., Karthik, S., Subramanian, K., and Ravikumar, V., "Origanum vulgare mediated biosynthesis of silver nanoparticle for its antibacterial and anticancer activity", Colloids Surf B, vol.108, pp.80– 84, 2013. [37] Kannan, N., Mukunthan, K.S., and Balaji, S., "A comparative study of morphology, reactivity and stability of synthesized silver nanoparticle useBacillus subtilis and Catharanthus roseus (L.) G. Don", Colloids Surf B, vol.86, pp.378–383, 2011.
[38] Gurusamy, A., and Cellapandian, K.., "Green Synthesis of Silver Nanoparticle useMillingtonia hortensis and Evaluation of their Antimicrobial Efficacy", Inter.j.nanomater.bios, vol.3 (1), pp.21-25, 2013.
[39] Raman, N., Sudharsan, S., Veerakumar, V., Pravin, N., and Vithiya, K., "Pithecellobium dulce mediated extra-cellular green synthesis of larvicidal silver nanoparticle", Spectrochim.Acta A.Mol.Biomo. Spectrosc, vol.96, pp.1031–1037, 2012.
[40] Thongnopkun, P., Jamkratoke, M., and Ekgasit, S., "Thermal behavior of nano silver clay in the application of handmade jewelry", Mater. Sci. Eng, vol.556, pp.849–854, 2012.
[41] Acemioglu, B., "Batch kinetic study of sorption of methylene blue by perlite", Chem. Eng. J, vol.106, pp.73–81, 2005.

[42] Langmuir, I., "The sorption of gases on plane faces of glass, mica and platinum", J. Am. Chem. Soc, vol.40, pp.1361–1403, 1918.
[43] Freundlich, H., "Uber die adsorption in loseungen", J. Phys. Chem, vol.57, pp.385– 470, 1907.
[44] Monika, J., Vinod Kumar, G., and Krishna, K., "Adsorption of hexavalent chromium from aqueous medium onto carbonaceous adsorbents prepared from waste biomassive", J. Hazard. Mater, vol.91, pp.949–954, 2010.
[45] Sheela, T., Arthoba Nayaka, Y., Viswanatha, R., Basavanna, S., and Venkatesha, T.G., "Kinetics and thermodynamics studies on the adsorption of Zn(II), Cd(II) and Hg(II) from aqueous solution useZ. oxide nanoparticle", Crushed.Technol, vol.217, pp.163–170, 2012.
[46] Hamid, G., Ahmad, M., Meisam, T., Parisa, Z., Mohammad Ghannadi, M., and Hossein Taheri, "Adsorption of Ag, Cu and Hg from aqueous solveuseexpanded perlite", J. Hazard. Mater, vol.177, pp.950–955, 2010.
[47] Wassana, Y., Cynthia, L., and Thanapol, S., "Displacementof intensive metals from aqueous systems with thiol workableized supermagnetic nanoparticle", Environ. Sci. technol, vol.41, pp.5114–5119, 2007.
[48] Yong, L., Xiaomei, S., and Buhai, L., "Adsorption of Hg2+ and Cd2+ by ethylenediamine modified peanut shells", Carbohydr.Polym, vol.81, 335-339, 2010.
[49] Shafey, E.I., "Displacementof Zn (II) and Hg (II) from aqueous solution on a carbonaceous sorbent chemically prepared from rice husk", J. Hazard.Mater, vol.175, pp.319-327, 2010.
[50] Smiciklas, I., Onjia, A., Raicevic, S., Janackovic, D., and Metric, M., "Factors influencing the displacementof divalent cationstech by hydroxyapatite", J. Hazard. Mater, vol.152, pp.876–884, 2008.
[51] McKay, G., and Ho, Y.S., "Pseudo-second order model for sorption processes", Process Biochem, vol.34, pp.451–465, 1999.
[52] Chen, Y.H., and Li, F.A., "Kinetic study on displacementof copper (II) usegoethite and hematite nano-photocatalysts", J. Colloid Interface Sci, vol.347, pp.277–281, 2010.
[53] Weber, W.J., and Morris, J.C., "Equilibria and capacities for adsorption on carbon", J. of Sanitary Engineering.Division, vol.90, pp.79–107, 1964.
[54] Ahmet, S., Mustafa, T., Demirhan, C., and Mustafa Soylak, "Equilibrium, kinetics and thermodynamic studies of adsorption of Pb (II) from aqueous solution onto Turkish kaolinite clay", J.Hazard. Mater, vol.149, pp.283–291, 2007.
[55] M.R. Karim, M.O. Aijaz, N.H. Alharth, H.F. Alharbi, F.S. Al-Mubaddel, M.R. Awual, Composite nanofibers membranes of poly (vinyl alcohol)/chitosan for selective lead (II) and cadmium (II) ionstech displacementfrom wastewater, Ecotox. Environ. Safety 169 (2019) 479–486. .
[56] Y. Kismir, A.Z. Aroguz, Adsorption characteristics of the hazardous dye Brilliant Green on Saklıkent mud, Chem. Eng. J. 172 (1) (2011) 199–206.

[57] A.M. Ahmed, M.I. Ayad, M.A. Eledkawy, M.A. Darweesh, E.M. Elmelegy, Displacementof iron, Z., and nickel-ionstech usenano bentonite and its applicationstech on power station wastewater, Heliyon 7 (2) (2021), e06315.
[58] K. Kaya, E. Pehlivan, C. Schmidt, M. Bahadir, Use of modified wheat bran for the displacementof chromium (VI) from aqueous solutionstech, Food Chem. 158 (2014) 112–117.
[59] N.E. Belkhouche, N. Benyahia, Modeling of adsorption of Bi (III) from Nit. medium by fattened resin D2EHPA/XAD-1180, J. Surf. Eng. Mater. Adv. Technol. 1 (2) (2011) 30–34.
[60] A.M. El-Sawy, H.A. Moa'mena, M.A. Darweesh, N.A. Salahuddin, Synthesis of modified $PANI/CQDs$ nanocomposite by dimethylgyloxime for displacementof $Ni\,(II)$ from aqueous solution, Face. Interface 26 (2021) 101392.